Bitlis Eren Üniversitesi Fen Bilimleri Dergisi
BİTLİS EREN UNIVERSITY JOURNAL OF SCIENCE
ISSN: 2147-3129/e-ISSN: 2147-3188
VOLUME: 13 NO: 3 PAGE: 519-529 YEAR: 2024
DOI:10.17798/bitlisfen.1328584

Biosorption of Methylene Blue into Pumpkin Seed: Isotherm, Kinetic and Thermodynamics Studies

İlhan KÜÇÜK[1*]

[1]*Rektorship, Muş Alparslan University, Muş, Türkiye*

(ORCID: 0000-0003-2876-3942)

Keywords: Biosorption, Methylene blue, Pumpkin seed, Kinetic, Isotherm.

Abstract

This work has demonstrated the potential utility of pumpkin seed shells (PSS) as a low-cost solid adsorbent for methylene blue (MB) adsorption. PSS have investigated surface functional groups with FTIR (after and before adsorption), crystal structure with XRD, and surface morphology with SEM-EDX. Biosorption parameters were examined contact time, pH, solution temperature, and initial concentration. This research was conducted to analyze adsorption processes involved in adsorption of MB onto crude PSS by gaining essential knowledge from the study of equilibrium adsorption kinetics, isotherms, and thermodynamics. It was determined whether four models-Langmuir, Temkin, Freundlich, and D-R models-fit experimental data derived from adsorption isotherms. In addition, the accuracy of fits of three models to experimental data derived from adsorption kinetics were tested, namely, the Elovich, pseudo-first order, and pseudo-second order models. Biosorption of MB on PSS is exothermic and spontaneous according to thermodynamic analysis. FTIR (Fourier transform infrared spectroscopy) studies show significant changes in the absorption values, shapes and positions of bands both before and after solute adsorption. It was found that there are two MB adsorption mechanisms: electrostatic attraction and hydrogen bonding

1. Introduction

Because of their harmful effects on a wide variety of life forms, dyes in wastewater are of great concern. Into the environment, the release of dyes raises both toxicological and esthetic issues. Industries such as plastics, leather, textiles, and paper use dyes to colour their products and consume a lot of water in the process. Consequently, they emerge a remarkable amount of colored wastewater [1]. It is well known that color has an important impact on how the public perceives water quality. Color is first contaminant in wastewater that can be detected. In water, even very low amounts of some dyes—less than 1 ppm— are undesirable and extremely visible [2]. Methylene blue dye (MB), with the molecular formula $C_{16}H_{18}N_3SCl$, also referred to as methyl thioninium chloride, is heterocyclic aromatic chemical substance. It falls under the cationic dye category. It is usually used dye for silk, wood, and cotton [3]. It may cause eye burns that can lead to permanent eye damage in both humans and animals. When ingested by mouth, it produces a burning sensation and may cause vomiting, nausea, mental confusion, excessive sweating, and methemoglobinemia. It can also cause brief, rapid, or laboured breathing when inhaled. Because of its adverse effects on receiving water, treatment of wastewater containing this dye is of great importance [4].

A variety of treatment methods is used to remove dyes from wastewater, including adsorption, integrated chemical-biological degradation, cation exchange

*Corresponding author: i.kucuk@alparslan.edu.tr
Received:17.07.2023, Accepted:15.08.2024

membranes, sonochemical degradation, micelle-assisted ultrafiltration, solar photo-Fenton, electrochemical degradation, fenton biological treatment scheme, integrated iron (III)-photo-assisted biological treatment, and biological processes [5,6]. Adsorption of synthetic dyes on affordable and effective solid supports was considered a cost-effective and simple method to remove them from wastewater and water, since conventional methods cannot effectively decolorize synthetic dyes in wastewater. A well-known equilibrium separation technique, adsorption is well suited for the decontamination of water. Compared to other methods of reusing water, adsorption has proven to be more advantageous due to its low initial cost, adaptability and ease of construction, and resistance to toxic pollutants. In addition, adsorption is not lead to formation of hazardous substances [7,8].

A biotechnological approach to sustainable development has a practical application branch, biosorption [9]. It is considered an economical, effective, and environmentally friendly method of water treatment. It keeps concentration of various water pollutants below limits recommended by various regulations. The principles of green chemistry are consistent with this protocol. It is important to understand the complex fundamentals of the biosorption process in terms of its various components. Shortly, it is metabolically independent process (passive uptake) based on the use of biowaste to remove various types of water pollutants [10]. The recycling of these biomasses (biowastes) generally brings a number of benefits. Their use in their natural or/and modified forms contributes directly to reduction of waste. Numerous ecological and environmental problems can be solved in this way. It is characterized by exceptional properties such as high efficiency and low operating and manufacturing costs [11].

The aim of this study is to utilize pumpkin seed, which can be considered as agricultural waste, as an adsorbent. Specifically, the focus is on the removal of pollutants such as methylene blue, which are harmful to human health and commonly used in industry, from aqueous environments. The research was conducted under various temperature conditions, different initial concentrations, varying contact times, and various pH levels. The impact of these factors ensured a detailed examination of their effects on the efficiency of methylene blue removal. Comprehensive experimental studies were conducted to determine important parameters such as the adsorption capacity and adsorption kinetics of pumpkin seed. The results highlight the potential of pumpkin seed husks as an effective adsorbent. This study not only presents an environmentally sustainable approach to waste management but also contributes to the development of new and effective treatment methods in fields such as water treatment industry.

2. Material and Method

2.1. Preparation of the biosorbent

The PSS were get from commercial (Muş/Turkey). The obtained pumpkin seeds had their interiors removed, and only the husks were utilized in this study. The pumpkin seeds were taken and dried in air until constant weight. They were then crushed with laboratory blender and sieved with 1.6-mm sieve. Pumpkin seed shells (PSS) remaining under the sieve were used as biosorbent

Figure 1. Pumpkin Seeds (Biosorbent)

2.2. Preparation of the adsorbate

0.5 g of methylene blue (Isolab C.I. 52015) was weighed and dissolved in 1liter of distilled water to prepare stock solution (500 ppm or 500 mg/L). The methylene blue solutions used in adsorption experiments were prepared by dilution from stock solution.

2.3. Adsorption procedure

In the isothermal experiments, fixed amount of GP (0.10 g) was added to five 100 mL erlenmeyer flasks containing 100 mL dilute solutions (10–50 mg/L). The Erlenmeyer flasks were capped and placed in water bath shaker, where they were shaken at 22, 30 and 40°C for 90 minutes. UV/vis spectrophotometer was used to measure final dye concentration in the solution at a maximum wavelength of 666 nm.

The kinetic tests followed a process almost identical to equilibrium tests. Aqueous samples were collected at predetermined times, and dye concentrations were assessed similarly.

The amount of MB at time qt, was calculated as follows:

$$q_t = \frac{(C_0 - C_t)V}{w} \quad (1)$$

2.3.1 Effect of contact time and initial concentration

Each 500 mL volume of MB solution contained 0.5 g of the PSS sample. Experiments were performed at 295 K for 90 minutes at initial dye solution concentrations of 30, 40, and 50 mg/L.

2.3.2 Effect of temperature

0.5 g of the PSS sample was added to each 500 mL volume of MB aqueous solution at initial concentration of 30 mg/L. Experiments were performed at 22, 30 and 40°C for 90 minutes.

2.3.3 Effect of pH

The solution's pH was studied at pH 2, 3, 4, 5, 6, 7, 8, 9, 10, 11, and 12. At a constant adsorption time of 90 minutes, 0.1 g of PSS sample was added to each 100 mL of the aqueous solution MB with initial concentration of 20 mg/L.

3. Results and Discussion

3.1. Characterization of adsorbent

3.1.1 FTIR analysis

Using ATR-FTIR spectroscopy, the surface chemistry of PSS was investigated both before and after MB adsorption. Both the surface groups of the PSS and the nature of the interactions between PSS and MB were investigated using ATR-FTIR spectroscopy. By comparing the IR spectra obtained after and before the interaction of MB with PSS, much can be learned about the interactions that take place. The ATR spectra of the biosorbent PSS are shown in Fig. 2 A. The hydroxyl group in lignin, hemicellulose, cellulose, and adsorbed water on the surface of adsorbent exhibits an O-H stretching vibration associated with broad peak at 3290 cm^{-1}. In general, the methoxyl groups in cellulose, lignin, hemicellulose, and aliphatic acids show symmetric and asymmetric C-H stretching vibrations, respectively, as indicated by the peaks at 2890 and 2865 cm^{-1} [12]. The band at 1742 cm^{-1} is due to stretching of carbonyl or carboxyl groups. Due to carboxylate and phenol groups in the chemical structures of aliphatic/phenolic carboxyl molecules, the peak at 1654 cm^{-1} was determined to be of intensity and width for C=C stretching in aromatic rings. C=C or C-O vibrations are responsible for peak at 1511 cm^{-1}, while aromatic C=C stretching vibrations occurred peaks at 1445 and 1226 cm^{-1} [13]. In carboxylate groups C-O stretching vibrations (alkyl groups and alkanes) are assumed to be responsible for observed peak at 1367 cm^{-1}. In spectral region, bands in 1030 cm^{-1}, which were present in all spectra with only slight variations in peak intensity and width, indicated presence of -glycosidic bonds in cellulose and hemicellulose and C-O stretching vibration of aliphatic ethers and alcoholic groups. Same bands also evidenced presence of general carboxyl groups, lactones, and lignin structure in the adsorbents of the study [14].

Based on the FTIR spectra indicating presence of -OH and C-O bonds of alcohols, esters, ethers, and phenols, on the surface of PSS the mechanism of MB adsorption was deduced. On surface of PSS, oxygen-containing functional groups (negatively charged or acidic groups) and dye species are electrostatically attracted to each other, in the adsorption process. Another possible component is hydrogen bonding contact between N atoms in the MB and H atoms on PSS surface. In addition, aromatic rings of MB and the hexagonal structure of PSS may interact as p-p electron donors and acceptors. This type of interaction was regularly observed when the dye MB was adsorbed onto various carbon-based materials [15].

3.1.2 XRD analysis

The crystalline morphology of PSS was examined by powder X-ray diffraction (Fig. 2 B). In XRD, the PSS shows distinct peaks at 2θ = 27.3, 31.6, 45.4, 56.4, 66.2, and 75.2. This clearly shows that the PSS has high crystallinity. The six peaks mentioned above have d-spacings of 3.27, 2.82, 1.99, 1.63, 1.41 and 1.26 A˚, respectively. These peaks are formed from NaCl in the structure (RRUFF ID: R070292.1. Crystal System: cubic). In addition to, one peak is existed at around 22° which is assigned to the reflection from the 200 planes. This peak consists of cellulose in the structure [16].

3.1.1 SEM analysis

In research, the PSS investigated by scanning electron microscopy (SEM). The SEM images of PSS and PSS-MB-loaded samples are shown in Fig. 3. They prove that the adsorption of the studied solutes changed the PSS structure. The PSS-MB-loaded samples tended to form spherical aggregates, as can be seen in the SEM micrographs. In addition, S atom was found in the structure after MB adsorption in

EDX analysis. This confirms that the structure adsorbs MB.

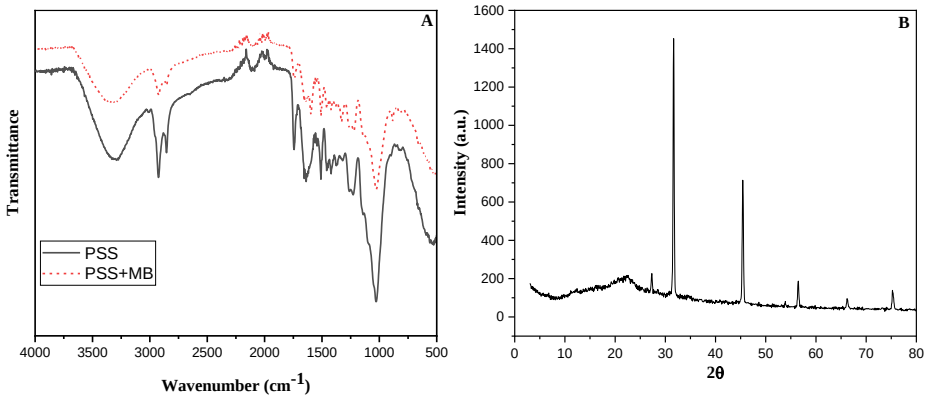

Figure 2. A. Fourier-transform infrared spectroscopy spectrum **B.** XRD spectrum

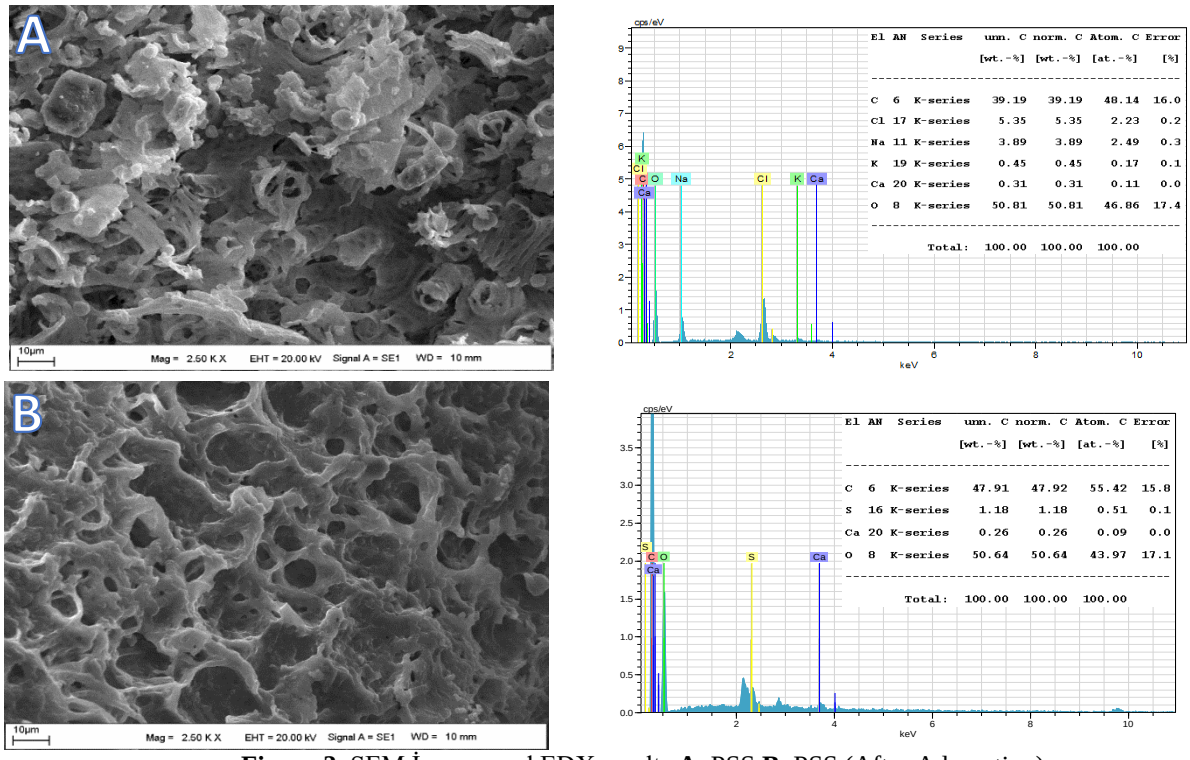

Figure 3. SEM İmages and EDX results **A.** PSS **B.** PSS (After Adsorption)

3.2. Adsorption Study

3.2.1 Effect of initial concentration and contact time

Fig. 4. A shows adsorption of dye MB on fixed amount of 0.5 g per 500 mL of PSS as a function of exposure time at a constant pH of 5.8. The dye MB

was initially rapidly adsorbed. Approximately half of the MB dye was absorbed in the first 5 minutes. Furthermore, the uptake of the dye MB gradually increased up to 90 minutes of increased contact time between adsorbent and adsorbate before reaching a plateau at a maximum update of 16 mg/g with 53.3% removal (initial concentration 30 mg/L). The rapid initial adsorption rate can be ascribed to increased number of active sites in the form of functional groups and pores on surface of PSS during the first phase of the adsorption process. The accumulation of dye molecules on surface of PSS causes adsorption process to proceed slowly because it stops the molecules from diffusing into the pores. In addition, initial concentration of pollutants in the system has a significant effect on adsorbent's ability to bind pollutants. In this situation, initial concentration of the MB was chosen between 30 mg/L and 50 mg/L. As shown in Fig. 4. A, the uptake of MB on PSS increased from 16 mg/g to 20.6 mg/g by changing initial concentration from 30 mg/L to 50 mg/L. Later, it was found that required equilibrium time for the MB increased with an increase in initial concentration.

3 .2.2 Effect of Temperature

Temperature is important and effective parameters in the adsorption process and affects both transfer process and adsorption kinetics of dye. In Fig. 4 B, impact of temperature on adsorption effectiveness of MB dyes was examined using PSS biosorbent in temperature range of 22 to 40 °C. The results demonstrated that when temperature increased from 22 °C to 40 °C, the adsorption efficiency of MB dye employing PSS biosorbent reduced from 53.3% to 48%. This shows that use of adsorbent in MB adsorption process is exothermic [17]. The increased solubility of MB in an aqueous solution causes interactions between dye molecule and solvent to be stronger than those between dye molecule and the adsorbent, which may lead to a decrease in efficiency of adsorption process with increasing temperature [18]. Therefore, PSS biosorbent was found to work best at a temperature of 22 °C for MB dye adsorption process.

3.2.3 Effect of pH

Capacity of PSS to remove MB was found to be more effective at higher pH values. Fig. 4. C shows the removal of MB for a study performed under 2-12 pH. The removal efficiency was lower at an acidic pH. This result shows that protonation of carbonyl and hydroxyl groups on surface of PSS repels positively charged MB ions and negatively affects removal efficiency. However, as pH increases, surface of PSS material becomes negatively charged, making it easier to attract and remove positively charged MB ions from water. Analysis of the pH_{pzc} can help confirm this conclusion. The calculated pH_{pzc} of PSS was 5.66 (Fig. 4. D). Consequently, the surfaces of these materials below this pH are known to be positively charged [19]. This confirms our earlier conclusion. Other researchers who studied the removal of MB from water using biomass reported a similar impact of pH on removal of MB [20]. MB increased with an increase in initial concentration.

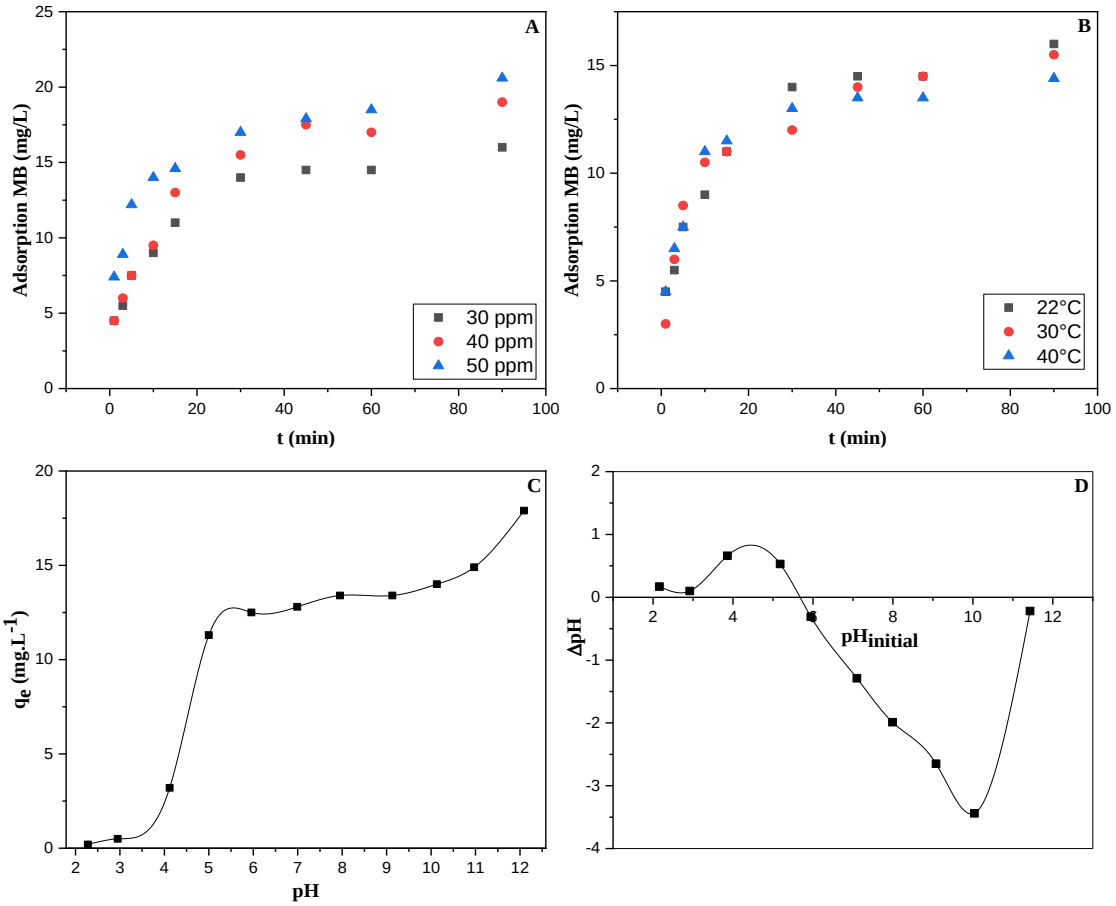

Figure 4. A. Effect of contact time and initial ion concentration of MB on PSS biosorbent **B.** Effect of temperature of MB on PSS biosorbent C_0= 30 mg/L **C.** Effect of solution pH of MB on PSS biosorbent **D.** pHpzc graph

3.2.4 Isotherm studies

Adsorption isotherm models explain the interactions between pollutants and adsorbents. To explain this interaction, isotherm models were investigated in research.

Langmuir isotherm model, defined to compare adsorption capacities and performances of different biosorbents, assumes single-layer adsorption. This isotherm model states that adsorption can only take place in a finite (constant) number of equal and equivalent localized patches that have lateral contact and are not steric [21]. Adsorption is not ideal, is reversible, and is not just confined to the creation of monolayers, according to the Freundlich isotherm. According to this model, the amount adsorbed represents the total amount of adsorption on all sites (each of which has a bond energy), with stronger binding sites being occupied first until the adsorption process is complete and the adsorption energy is exponentially reduced [21]. The Temkin isotherm model takes into account interactions between adsorbate and adsorbent assumes that the heat of adsorption (temperature function) decreases linearly rather than logarithmically with coating. This model does not take into account extremely low and high values of the concentrations [22]. Nonlinear equations of Langmuir, Freundlich, and Temkin are shown in Eq. 2,3,4 respectively.

$$q_e = \frac{q_m K_L C_e}{1 + K_L C_e} \quad (2)$$

$$q_e = K_F C_e^{\frac{1}{n}} \quad (3)$$

$$q_e = B_T \ln(A_T C_e) \quad (4)$$

The experimental data were applied to isotherm equations, and graphs shown in Fig. 5 A were obtained. Isotherm constants were calculated using obtained graphs and listed in Table 1.

Equilibrium concentration of adsorbate, C_e (mg/L), amount of dye adsorbed per gram of adsorbent at equilibrium, q_t (mg/g), maximum monolayer coverage capacity, q_m (mg/g), initial concentration,

C_0, constant related to energy of adsorption (Langmuir Constant), K_L (L/mg), Freundlich isotherm constant, K_F (mg/g)/(mg/L)^n, adsorption intensity, A_T(L/g), Temkin isotherm constant, n, Temkin isotherm equilibrium binding constant, B_T (j/mol).

Table 1 lists constants for the Langmuir model, which were determined. Other important parameter defining properties of the Langmuir model is the adsorption intensity (R_L). This parameter determines mode and quality of isothermal model. Respectively, for $R_L > 1$, $R_L = 0$, $R_L = 1$ and $0 > R_L > 1$, the adsorption process is undesirable, irreversible, linear, and favorable, [23]. R_L value of the adsorption process of MB, which ranged from 0 to 1, was in the ideal range. Adsorption capacities of MB were calculated at 38.6.

Table 1 lists the constants for the Freundlich model, which were determined. While 1/n is a function of strength of adsorption in adsorption process, the constant K_F is a rough measure of adsorption capacity. Separation between two phases is independent of concentration when n = 1. Normal adsorption occurs when the value of 1/n is less than one. On the other hand, cooperative adsorption is indicated when 1/n is greater than one. When the pressure increases without constraints, the function reaches an asymptotic maximum. The constants K_F and n change with temperature to account for empirical finding that adsorbed amount increases more slowly and larger pressures are required to saturate surface. However, linear regression is often used to determine parameters of the kinetic and isothermal models, while K_F and n are parameters specific to the system of sorbentand sorbate and must be determined by data fitting. Because 1/n is heterogeneity parameter and smaller 1/n is, higher predicted heterogeneity, linear least squares approach and linear transformed equations is usually used to correlate sorption data. When 1/n = 1, this formula simplifies to a linear adsorption isotherm. A favorable sorption process is given when n is between one and ten. According to the data in Table 3, the biosorption of MP is favorable, and the R^2 value is 0.978, with the value of 1/n = 0.6, when n=1.66.

Table 1 lists constants for Temkin model, which were determined. The equilibrium binding constant of Temkin isotherm is A_T, while the heat constant of sorption (J/mol) is B_T. A_T = 0.47 L/g, B = 8.51, J/mol, a measure of the heat of sorption, and R^2 = 0.996 indicate a physical adsorption process.

Table 1. The parameters of the selected adsorption isotherm models obtained from Fig. 5.

Langmuir		**Freundlich**		**Temkin**	
$\mathbf{q_m}$	38.6	$\mathbf{K_F}$	3.06	$\mathbf{B_T}$	8,51
$\mathbf{K_L}$	0.04	**n**	1.66	$\mathbf{A_T}$	0.47
$\mathbf{R^2}$	0,993	$\mathbf{R^2}$	0.978	$\mathbf{R^2}$	0.996

3.2.5 Kinetics studies

Adsorption kinetics of MB onto PSS were investigated using pseudo-first-order (PFO), pseudo-second-order (PSO), Elovic, and intraparticle diffusion methods.

PFO model equation is applied to adsorption in a liquid-solid system. In this equation, the differences in saturation levels of concentration are directly proportional to adsorbate uptake [24]. The PFO model equation is known as follows:

$$q_t = q_e(1 - \exp(-k_1\, t)) \quad (5)$$

Chemisorption is usually described by pseudo-second-order (PSO) model and Elovich model. More specifically, The pseudo-second-order model depicts the participation of valence forces through the exchange of electrons between the adsorbate and the adsorbent as covalent forces and ion exchange, whereas the Elovich model explains the kinetics of chemisorption on an adsorbent with a heterogeneous surface [21]. The PSO model and Elovich equation are respectively known as follows:

$$q_t = \frac{q_e^2 k_2 t}{1 + k_2 q_e t} \quad (6)$$

$$q_t = \frac{1}{b} In(abt + 1) \quad (7)$$

The rate-limiting step in the adsorption process is intraparticle diffusion, which produces a straight line when plotting amount of metal ions adsorbed against square root of contact time. [25]. For an adsorption system, the following is intraparticle diffusion equation that is most frequently used.

$$q_t = k_p t^{1/2} + C \quad (8)$$

q_t (mg g^{-1}) is adsorption capacity at time t and k_1 (min^{-1}) is rate constant of the pseudo-first order adsorption. Rate constant of pseudo-second order adsorption, k_2 (g mg^{-1} min^{-1}). k_p (mg g^{-1} $min^{-1/2}$) is intraparticle diffusion rate constant and C (mg g^{-1}) is a constant. a (mg/g ·min) is initial adsorption rate, and the desorption constant, b, depends on amount of surface covering and the chemisorption's activation energy.

Based on higher R^2 values compared to PFO and PSO models, the results show that adsorption process of the dye MB follows Elovich model. The results show that a chemisorption mechanism controls the adsorption of the dye MB by PSS. Additionally, the qe value closest to the C_0 values was determined in the PSO model. Fig. 5 D and Table 2 contain the plots and the analyzed parameters of intraparticle diffusion, respectively. In Fig. 5 D, a linearity segment can be seen, indicating that the only rate-regulating phase in adsorption process was intraparticle diffusion of dye MB by PSS.

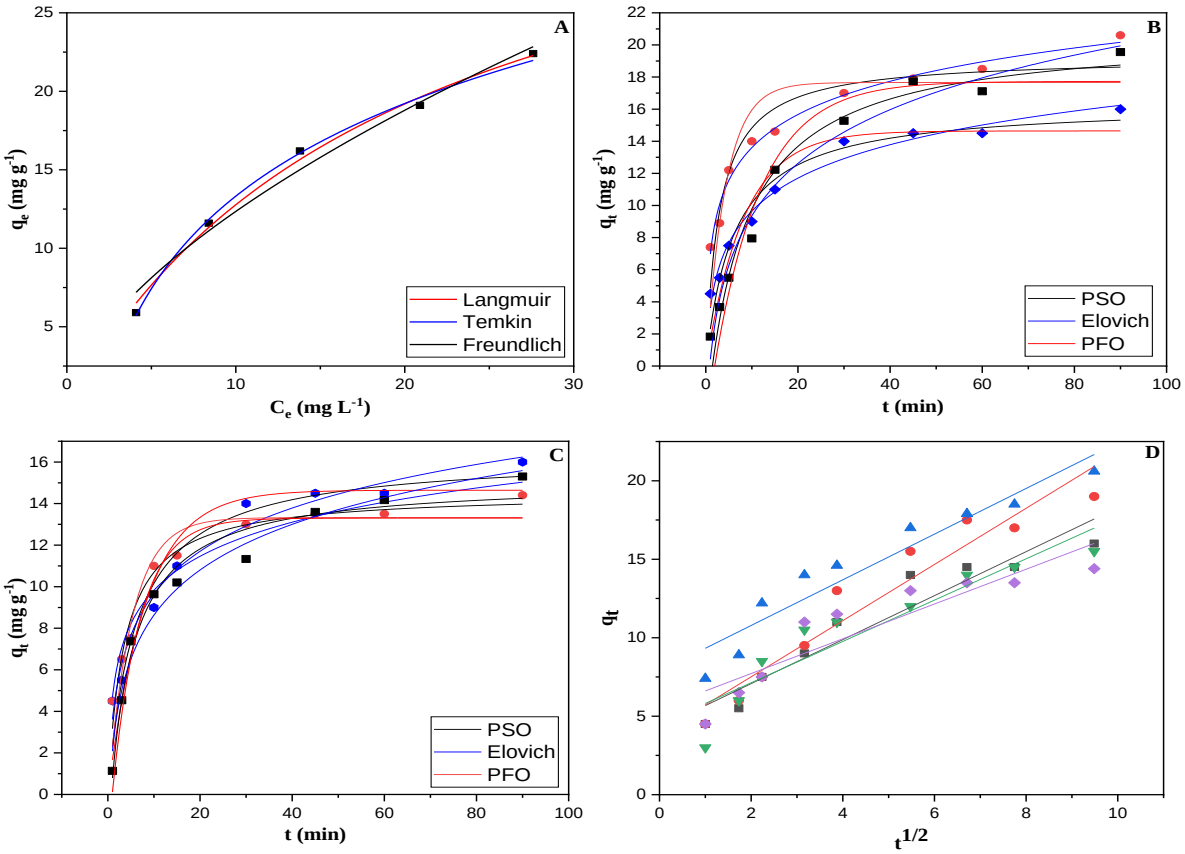

Figure 5. A. Isotherm models **B.** Kinetic models of the initial concentration **C.** Kinetic models of the temperature **D.** Intraparticle Diffusion

Table 2. The parameters of the selected adsorption kinetic models at different solution temperatures and initial concentration.

		Pseudo-First Order			**Pseudo-Second Order**		
°C	**C_0**	**k_1**	**q_e**	**R^2**	**k_2**	**q_e**	**R^2**
22	30	0.12	14.6	0.897	0.01	16.3	0.949
22	40	0.09	17.5	0.927	0.006	20	0.960
22	50	0.23	17.6	0.786	0.017	19.23	0.910
30	30	0.16	13.7	0.918	0.013	15.3	0.974
40	30	0.19	13.3	0.919	0.019	14.5	0.969
		Elovich			**Intraparticle Diffusion**		
°C	**C_0**	**a**	**b**	**R^2**	**k_p**	**C**	**R^2**
22	30	6.90	0.32	0.976	1.40	4.27	0.915
22	40	5.18	0.24	0.975	1.79	3.93	0.927
22	50	27.6	0.33	0.983	1.45	7.87	0.914
30	30	14.5	0.41	0.962	1.31	4.49	0.869
40	30	8.15	0.35	0.978	1.10	5.50	0.825

3.2.4 Thermodynamics of adsorption

Adsorption capacity of adsorbents and transport/kinetic mechanism of adsorption are significantly affected by temperature. The following equations 10 and 11 were used to calculate the thermodynamic parameters, adsorption free energy (ΔG°), standard enthalpy (ΔH°) and entropy changes (ΔS°).

$$\Delta G° = -RT\ln(K_c) \quad (10)$$

K_c was calculated as follows: Langmuir constant multiplied by the molar mass of methylene blue, then multiplied by the molecular mass of methylene blue, and finally multiplied by 1000. R (8.314 $JK^{-1}mol^{-1}$) is universal gas constant, T(K) is temperature. ΔS° and ΔH° values were calculated with the Van't Hoff (eq. 21).

$$\ln K_C = \frac{\Delta S^0}{R} - \frac{\Delta H^0}{RT} \quad (11)$$

Table 3, the thermodynamic parameters are shown. Positive value of ΔG° indicates unspontaneous nature of adsorption of MB onto PSS surface at given experimental conditions [26]. Exothermic character of adsorption process is shown by negative enthalpy (ΔH°) of process. The decrease randomness at solid/liquid boundary during dye adsorption on PSS is shown by the negative value of ΔS° [27].

Table 3. Thermodynamic parameters

ΔG° (kJ/mol)			ΔH° (kJ/mol)	ΔS° (kJ/mol·K)
22°C	30°C	40°C		
23.618	22.294	21.859	-53.237	-0.101

4. Conclusion and Suggestions

In this study, cheap, renewable, and waste material pumpkin seed shells were used as an adsorbent. Methylene blue, which is used in many sectors and pollutes the environment, was selected as the adsorbate. The study aimed to determine kinetic and isotherm properties of adsorbent. The parameters of pH, initial concentration, temperature, and contact time were investigated for removal of methylene blue. Although a significant increase in initial concentration, pH, and contact time was observed, the removal of methylene blue decreased with increasing temperature. This decrease was confirmed by a thermodynamic study, which established that biosorption is an exothermic process. The obtained results were applied to different isotherm models, and the Temkin model (R2= 0.996) was found to be the most suitable. Kinetic studies demonstrated that biosorption followed Elovich model (R2=0.983). Consistent with these results, it was concluded that pumpkin seed shells can be effectively used as a renewable adsorbent.

Statement of Research and Publication Ethics

The study is complied with research and publication ethics

References

[1] Y. Zhou, J. Lu, Y. Zhou, and Y. Liu, "Recent advances for dyes removal using novel adsorbents: A review," *Environ. Pollut.*, vol. 252, pp. 352–365, 2019.

[2] M. Rafatullah, O. Sulaiman, R. Hashim, and A. Ahmad, "Adsorption of methylene blue on low-cost adsorbents: A review," *J. Hazard. Mater.*, vol. 177, no. 1–3, pp. 70–80, 2010.

[3] A. M. Elgarahy, K. Z. Elwakeel, S. H. Mohammad, and G. A. Elshoubaky, "A critical review of biosorption of dyes, heavy metals and metalloids from wastewater as an efficient and green process," *Clean. Eng. Technol.*, vol. 4, no. 100209, p. 100209, 2021.

[4] Y. Wang, Q. Peng, N. Akhtar, X. Chen, and Y. Huang, "Microporous carbon material from fish waste for removal of methylene blue from wastewater," *Water Sci. Technol.*, vol. 81, no. 6, pp. 1180–1190, 2020.

[5] M. Onay and Ç. Sarici Özdemir, "Equilibrium studies for dye adsorption onto Red Clay," *Naturengs MTU Journal of Engineering and Natural Sciences Malatya Turgut Ozal University*,vol.3, no. 2, pp. 36-45, 2022.

[6] N. Kaya, Z. Yıldız, and S. Ceylan, "Preparation and characterisation of biochar from hazelnut shell and its adsorption properties for methylene blue dye," *J. Polytech*., vol. 21, no. 4, pp. 765-776, 2018.

[7] S. Savcı and F. Karadağ, "Fast adsorption of methylene blue by filter coffee waste," *NWSA-Eng. Sci*., vol. 15, no. 4, pp. 111–120, 2020.

[8] Z. Ciğeroğlu and E. Yildirir, "Vermicompost as a Potential Adsorbent for the Adsorption of Methylene Blue Dye from Aqueous Solutions," *JOTCSA*, vol. 7, no. 3, pp. 893–902, 2020.

[9] T. Satır and İ. Erol, "Calcined Eggshell for the Removal of Victoria Blue R Dye from Wastewater Medium by Adsorption," *JOTCSA*, vol. 8, no. 1, pp. 31–40, 2021.

[10] V. Krstić, T. Urošević, and B. Pešovski, "A review on adsorbents for treatment of water and wastewaters containing copper ions," *Chem. Eng. Sci*., vol. 192, pp. 273–287, 2018.

[11] N. K. Gupta, A. Gupta, P. Ramteke, H. Sahoo, and A. Sengupta, "Biosorption-a green method for the preconcentration of rare earth elements (REEs) from waste solutions: A review," *J. Mol. Liq*., vol. 274, pp. 148–164, 2019.

[12] A. Stavrinou, C. A. Aggelopoulos, and C. D. Tsakiroglou, "Exploring the adsorption mechanisms of cationic and anionic dyes onto agricultural waste peels of banana, cucumber and potato: Adsorption kinetics and equilibrium isotherms as a tool," *J. Environ. Chem. Eng*., vol. 6, no. 6, pp. 6958–6970, 2018.

[13] K. Komnitsas, D. Zaharaki, I. Pyliotis, D. Vamvuka, and G. Bartzas, "Assessment of pistachio shell biochar quality and its potential for adsorption of heavy metals," *Waste Biomass Valorization*, vol. 6, no. 5, pp. 805–816, 2015.

[14] D. Angın, T. E. Köse, and U. Selengil, "Production and characterization of activated carbon prepared from safflower seed cake biochar and its ability to absorb reactive dyestuff," *Appl. Surf. Sci*., vol. 280, pp. 705–710, 2013.

[15] B. Hu et al., "Efficient elimination of organic and inorganic pollutants by biochar and biochar-based materials," *Biochar*, vol. 2, no. 1, pp. 47–64, 2020.

[16] Z. Zhang, M. Zhu, and D. Zhang, "A Thermogravimetric study of the characteristics of pyrolysis of cellulose isolated from selected biomass," *Appl. Energy*, vol. 220, pp. 87–93, 2018.

[17] M. Naushad, A. A. Alqadami, Z. A. AlOthman, I. H. Alsohaimi, M. S. Algamdi, and A. M. Aldawsari, "Adsorption kinetics, isotherm and reusability studies for the removal of cationic dye from aqueous medium using arginine modified activated carbon," *J. Mol. Liq*., vol. 293, no. 111442, p. 111442, 2019.

[18] R. Foroutan, S. J. Peighambardoust, S. H. Peighambardoust, M. Pateiro, and J. M. Lorenzo, "Adsorption of crystal Violet dye using activated carbon of lemon wood and activated carbon/Fe3O4 magnetic nanocomposite from aqueous solutions: A kinetic, equilibrium and thermodynamic study," *Molecules*, vol. 26, no. 8, p. 2241, 2021

[19] S. Manna, D. Roy, P. Saha, D. Gopakumar, and S. Thomas, "Rapid methylene blue adsorption using modified lignocellulosic materials," *Process Saf. Environ. Prot*., vol. 107, pp. 346–356, 2017.

[20] P. M. Thabede, N. D. Shooto, and E. B. Naidoo, "Removal of methylene blue dye and lead ions from aqueous solution using activated carbon from black cumin seeds," *S. Afr. J. Chem. Eng*., vol. 33, pp. 39–50, 2020.

[21] M. Choudhary, R. Kumar, and S. Neogi, "Activated biochar derived from Opuntia ficus-indica for the efficient adsorption of malachite green dye, Cu+2 and Ni+2 from water," *J. Hazard. Mater*., vol. 392, no. 122441, p. 122441, 2020.

[22] K. Y. Foo and B. H. Hameed, "Insights into the modeling of adsorption isotherm systems," *Chem. Eng. J.*, vol. 156, no. 1, pp. 2–10, 2010.

[23] E. Ajenifuja, J. A. Ajao, and E. O. B. Ajayi, "Adsorption isotherm studies of Cu (II) and Co (II) in high concentration aqueous solutions on photocatalytically modified diatomaceous ceramic adsorbents," *Appl. Water Sci.*, vol. 7, no. 7, pp. 3793–3801, 2017.

[24] J. Wang and X. Guo, "Adsorption kinetic models: Physical meanings, applications, and solving methods," *J. Hazard. Mater.*, vol. 390, no. 122156, p. 122156, 2020.

[25] A. Pholosi, E. B. Naidoo, and A. E. Ofomaja, "Intraparticle diffusion of Cr(VI) through biomass and magnetite coated biomass: A comparative kinetic and diffusion study," *S. Afr. J. Chem. Eng.*, vol. 32, pp. 39–55, 2020.

[26] P. Nautiyal, K. A. Subramanian, and M. G. Dastidar, "Kinetic and thermodynamic studies on biodiesel production from Spirulina platensis algae biomass using single stage extraction–transesterification process," *Fuel (Lond.)*, vol. 135, pp. 228–234, 2014.

[27] M. Toprak, A. Salci, and A. R. Demirkiran, "Comparison of adsorption performances of vermiculite and clinoptilolite for the removal of pyronine Y dyestuff," *React. Kinet. Mech. Catal.*, vol. 111, no. 2, pp. 791–804, 2014.